

# Increasing the Net Charge and Decreasing the Hydrophobicity of Bovine Carbonic Anhydrase Decreases the Rate of Denaturation with Sodium Dodecyl Sulfate

Katherine L. Gudiksen, Irina Gitlin, Demetri T. Moustakas, and George M. Whitesides

Department of Chemistry and Chemical Biology, Harvard University, Cambridge, Massachusetts 02138

**ABSTRACT** This study compares the rate of denaturation with sodium dodecyl sulfate (SDS) of the individual rungs of protein charge ladders generated by acylation of the lysine  $\epsilon$ -NH<sub>3</sub><sup>+</sup> groups of bovine carbonic anhydrase II (BCA). Each acylation decreases the number of positively charged groups, increases the net negative charge, and increases the hydrophobic surface area of BCA. This study reports the kinetics of denaturation in solutions containing SDS of the protein charge ladders generated with acetic and hexanoic anhydrides; plotting these rates of denaturation as a function of the number of modifications yields a U-shaped curve. The proteins with an intermediate number of modifications are the most stable to denaturation by SDS. There are four competing interactions—two resulting from the change in electrostatics and two resulting from the change in exposed hydrophobic surface area—that determine how a modification affects the stability of a rung of a charge ladder of BCA to denaturation with SDS. A model based on assumptions about how these interactions affect the folded and transition states has been developed and fits the experimental results. Modeling indicates that for each additional acylation, the magnitude of the change in the activation energy of denaturation ( $\Delta\Delta G^\ddagger$ ) due to changes in the electrostatics is much larger than the change in  $\Delta\Delta G^\ddagger$  due to changes in the hydrophobicity, but the intermolecular and intramolecular electrostatic effects are opposite in sign. At the high numbers of acylations, hydrophobic interactions cause the hexanoyl-modified BCA to denature nearly three orders of magnitude more rapidly than the acetyl-modified BCA.

## INTRODUCTION

### Background

Interactions of proteins with surfactants are important in biochemistry, but incompletely understood. Probably the most common example of the use of protein-surfactant interactions in biochemistry is SDS-polyacrylamide gel electrophoresis (SDS-PAGE) (1), a technique used to separate proteins based on their molecular weight. Other examples of the use of surfactants in protein science include the solubilization and reconstitution of membrane-associated proteins by detergents (2–4), and stabilization of drugs (5–7).

The aggregates formed between proteins and SDS have been investigated extensively, but their structures, and the mechanism by which they are formed, still have not been established unambiguously. When fully denatured in SDS, proteins bind  $\sim 1.4$  g of SDS per g of protein (or  $\sim 1$  SDS molecule per 2 amino acids) (8–11). A wide variety of models has been proposed for the structure of the denatured protein-SDS aggregate (12,13):

- i. In the “rod-like model” (10), the SDS molecules form a shell along the length of the protein backbone.
- ii. In the “pearl necklace model” (14), micelle-like structures of SDS are scattered along the chain of the denatured protein. The protein passes through micelles of approximately constant size.

- iii. In the “flexible  $\alpha$ -helix/random coil model” (15), SDS increases the propensity of cationic residues to form  $\alpha$ -helices.
- iv. In the “flexible-helix model” (16), the detergent molecules form a flexible, capped cylindrical micelle, around which the hydrophilic segments of the polypeptide associate. The major stabilizing interaction in this model is hydrogen bonding between the oxygen atoms in the SDS molecules and the nitrogen atoms of the polypeptide backbone.
- v. In the “protein decorated micelle model” (12), the protein is located on the outside of micelles of differing sizes.

All these models aim to explain the observation of a constant ratio of SDS molecules to the number of amino acids in the protein-SDS aggregates, but experimental results have not been able to distinguish conclusively between them.

Recent work (17) strongly suggests that molecules of SDS that are associated with the protein are organized into micelles. It appears that either the pearl necklace or protein decorated micelle model is the most accurate of the five models for the protein-SDS aggregate. For bovine serum albumin (BSA), Turro et al. (18) showed, using NMR, that the mobility of the sulfate headgroups was very small and concluded that BSA is coiled predominantly around the exterior of the bound SDS molecules. For this protein, the most likely structure of the protein-SDS aggregate was the protein-decorated micelle. Xu and Keiderling (19) studied the acid-denatured state of cytochrome *c* and showed that, at high concentrations of SDS (0.5 M), some of the protein was

Submitted January 19, 2006, and accepted for publication March 22, 2006.

Address reprint requests to George M. Whitesides, Tel.: 617-495-9430; Fax: 617-495-9857; E-mail: [gwhitesides@gmwgroup.harvard.edu](mailto:gwhitesides@gmwgroup.harvard.edu).

© 2006 by the Biophysical Society

0006-3495/06/07/298/13 \$2.00

doi: 10.1529/biophysj.106.081547

located inside micelles (the pearl necklace model) whereas some of the protein remained on the surface of micelles (protein decorated micelle model).

Regardless of the structure of the aggregate, both the mechanism of denaturation and the contributions of electrostatic and hydrophobic interactions to the denaturation of proteins by SDS remain incompletely understood. Many groups have used equilibrium dialysis and calorimetry (20–23) to demonstrate that at low concentrations of SDS, the average number ( $\bar{\nu}$ ) of SDS molecules bound to a protein molecule increases sharply as the SDS concentration is raised. The binding then reaches a plateau near values of  $\bar{\nu}$  roughly equal to the number of cationic residues in the protein, and increases sharply again as the SDS concentration approaches the critical micelle concentration (cmc) (13). At low concentrations of SDS, the binding is mainly electrostatic, with some simultaneous interaction of the hydrophobic tail with nearby hydrophobic patches on the protein. These initial interactions presumably cause some protein unfolding and expose additional hydrophobic sites. More SDS molecules then bind to the exposed hydrophobic sites in the protein-SDS aggregate (24,25).

Although the overall picture described by these theories is probably qualitatively correct, the mechanistic details almost certainly differ among proteins, and the distinction made between the two regimes—primarily electrostatic, and primarily hydrophobic—is probably blurred in many cases. The objective of this study was to distinguish between the effects of charge and of hydrophobicity on the kinetics of denaturation of a model protein, bovine carbonic anhydrase (BCA, E.C. 4.2.1.1), and of derivatives of this protein generated by acylation, having different charges and hydrophobicities.

## EXPERIMENTAL DESIGN

### BCA is a good model for studying processes involving denaturation

BCA is easy to handle, monomeric, and commercially available; it has no disulfide bonds (26,27). Its structure is well-defined by x-ray crystallography (28,29), and its binding of arylsulfonamide inhibitors is also structurally well-defined (30). A wide range of those inhibitors is commercially available and synthetically accessible. There is an extensive literature describing the denaturation of BCA with other denaturants, i.e., urea and guanidinium chloride (GuHCl) (31–40). These studies showed that the rate of folding of BCA is determined by the isomerization of proline residues (35,41), that BCA is not completely unfolded, even in saturated solutions of GuHCl (39,42, 43), and that BCA, like many proteins that have a large fraction of its structure in  $\beta$ -sheets, is particularly susceptible to aggregation in the partially (un)folded state (44–46).

The denaturation and renaturation of BCA with SDS is well-characterized: it is reversible at low concentrations of SDS (<0.1 mM), and easily followed by capillary electro-

phoresis (CE) (47,48). Yang et al. (49) synthesized a derivative of BCA, BCA-Ac<sub>18</sub> (all 18 lysine groups acetylated), in which the tertiary structure of the proteins is indistinguishable (by catalysis and circular dichroism) from the native structure, but where the external surface of the proteins lacks all 18 of the positively charged lysine  $\epsilon$ -NH<sub>3</sub><sup>+</sup> groups present in the native protein. After denaturation with SDS, both BCA and BCA-Ac<sub>18</sub> refold with similar rates (11  $\pm$  1 min for BCA and 21  $\pm$  2 min for BCA-Ac<sub>18</sub>) (50) to the same (native) structure upon complete removal of the SDS.

In a previous study, we demonstrated that the Zn(II) cofactor of CA does not complicate studies of refolding of CA (48). The Zn(II) cofactor is not required for refolding into a native-like conformation, does not remain associated with the unfolded protein, and does not significantly change the rate of refolding. The presence of the Zn(II) cofactor during refolding, however, does increase the total amount of recovered protein by a factor of 2. All of the solutions used in this study contain 100- $\mu$ M Zn(II), so that any folded BCA or BCA-derivative contains the Zn(II) cofactor (and therefore binds inhibitors).

### Protein charge ladders: systematic variation of protein charge

Reaction of BCA with limited quantities of an anhydride converts some of the 18 lysine- $\epsilon$ -NH<sub>3</sub><sup>+</sup> groups to lysine- $\epsilon$ -NHCOR groups. The derivatives appear in CE as a set of peaks with regular spacing, a protein charge ladder (51,52). Each “rung” of the charge ladder (with the exception of the native and completely acylated forms) is, we assume, a set of regioisomers with the same number, but different distribution, of modified lysine residues, and therefore, approximately the same net charge. Charge ladders are thus a family of derivatives of a protein, in which the charge can be changed systematically. Using different acylating reagents, we can independently vary another parameter—hydrophobicity—and use the charge to count the number of modifications. Variation in the extent of acylation, and in the structure of the acylating reagent, allow charge and hydrophobicity to be changed independently.

### Comparison of rates of denaturation of acetyl- and hexanoyl-charge ladders of BCA

In this study, we compare the rates of denaturation of two charge ladders of BCA, one prepared with acetic anhydride, (CH<sub>3</sub>CO)<sub>2</sub>O (BCA-Ac<sub>n</sub>), and one prepared with hexanoic anhydride, (CH<sub>3</sub>(CH<sub>2</sub>)<sub>4</sub>CO)<sub>2</sub>O (BCA-Hex<sub>n</sub>). We studied the kinetics of denaturation of both for two reasons: i), because the kinetics of interaction of proteins and surfactants represents an unexplored area; and, ii), practically, because we were unable to measure the equilibrium constants between native and denatured states for BCA and the members of the

charge ladders; the rates of denaturation and renaturation are intractably slow at the intermediate (1–2.5 mM) concentrations of SDS that would be required for equilibration (47). In addition, another process, presumably aggregation of partially folded intermediates, occurs at low concentrations of SDS (0.7–2.5 mM) and prevents equilibration of the folded and denatured states (47).

All members of the charge ladders used in this study are stable at room temperature in the absence of denaturant. Each rung of both of the charge ladders used here binds sulfonamide inhibitors (53) ( $K_d \sim 0.3$ – $1.3$  mM, Fig. S1, Supplementary Material). We conclude that all of the rungs retain a common active-site structure, and, we presume, a common tertiary structure.

For any charge ladder of BCA, as the number of modifications ( $n$ ) increases, the total charge on the protein becomes more negative, and the surface of the protein becomes more hydrophobic due to conversion of  $\text{NH}_3^+$  groups to NHCOR groups. Native BCA has a charge of  $\sim -2.9$  at pH 8.4 (50). The charge on the early rungs of the ladder increases linearly with the number of acylations; each rung adds an additional charge of  $\sim -0.9$  (54,55). Therefore, for example, BCA-Ac<sub>8</sub> has a charge of  $\sim -10$ . The later rungs of the ladder may differ by  $<0.9$  units of charge (56). Using the Linderstrøm-Lang model of cooperativity in proton binding (57), we calculated the charge on BCA-Ac<sub>18</sub> to be  $-19$  (50). The mobility of a given rung of BCA-Ac <sub>$n$</sub>  has nearly the same mobility as the corresponding rung of BCA-Hex <sub>$n$</sub> . We therefore assume that the charges of the BCA-Hex <sub>$n$</sub>  are indistinguishable from those of BCA-Ac <sub>$n$</sub>  for a given rung number. (Small deviations in mobility between later rungs of the two ladders may be due either to a change in charge or a change in drag between the two ladders. We assume that any differences in the mobilities are due to additional drag from the hexanoyl groups relative to the acetyl groups.)

Hydrophobicity parameters (Hansch  $\pi$ -parameters,  $\log P$ -values) are often used to quantify the hydrophobicity of modifications to molecules (59). The change in hydrophobicity from  $\text{NH}_3^+$  ( $\log P = -2.12$ ) (60) to  $\text{NHCOCH}_3$  (one modification using acetic anhydride,  $\log P = -1.21$ ) (61,62) is  $+0.9$ , that is, more hydrophobic. The change in  $\log P$  for the change from  $\text{NH}_3^+$  to  $\text{NH}(\text{COCH}_2)_4\text{CH}_3$  (one modification with hexanoic anhydride) is  $+2.9$  (62).

### Capillary electrophoresis

We use capillary electrophoresis to monitor the denaturation of charge ladders of BCA. As the negatively charged SDS molecules interact with the proteins, the electrophoretic mobility of the complex increases above that of BCA-Ac<sub>18</sub>; all of the rungs of both of the ladders have indistinguishable mobilities when they are denatured with SDS. Because the mobilities of the denatured proteins—fully associated with SDS—are much larger than the mobilities of any folded proteins, we can observe all of the rungs of the charge ladder

and the denatured protein in the same sample. We detect proteins using absorption at 214 nm; at this wavelength, the amide bonds and aromatic side chains of the protein absorb, but the SDS is transparent. Thus, there is no interference from micelles of SDS, and CE can be used with SDS both above and below the cmc.

### Model of the kinetics of the interaction of charge ladders of BCA with SDS

We interpret the kinetics of denaturation using transition state theory (Eq. 1). In this equation, we can relate the experimentally measured rate ( $k$ ) to the activation energy ( $\Delta G^\ddagger$ ), or the

$$k = \nu \kappa_{\text{TST}} e^{-\Delta G^\ddagger / RT} \quad (1)$$

difference in energy between the folded, starting state, and the conformations in the saddle point of the reaction. In Eq. 1,  $\nu$  is a characteristic vibration frequency along the reaction coordinate at the saddle point and  $\kappa_{\text{TST}}$  is a transmission coefficient. For simple chemical reactions,  $\kappa_{\text{TST}}$  is often assumed to be 1; that is, all of the molecules passing through the transition state proceed to product, and  $\nu = k_{\text{B}}T/h$  ( $\sim 6 \times 10^{12} \text{ s}^{-1}$ ) where  $k_{\text{B}}$  is the Boltzmann constant,  $T$  is the temperature, and  $h$  is the Planck constant. For protein folding, however, the transmission through the saddle point is believed to be much less than unity. An empirical estimate for  $\nu \kappa_{\text{TST}}$  in the folding of proteins is  $10^6 \text{ s}^{-1}$  (62,63). This number was calculated for cytochrome *c* ( $t_{\text{folding}} \cong 400 \text{ ms}$ ) (64) and is, probably, an underestimate for BCA because it is a larger protein than cytochrome *c* and folds much more slowly ( $t_{\text{folding}} \cong 10 \text{ min}$ ) (50,65,66). Assuming that  $\nu \kappa_{\text{TST}}$  does not change with type or number of acylation, an incorrect estimate for  $\nu \kappa_{\text{TST}}$  will affect only the scale of  $\Delta G^\ddagger$ . An underestimate in the value of  $\nu \kappa_{\text{TST}}$  will lead to an overestimate in the value of  $\Delta G^\ddagger$ .

### Qualitative description of the model of SDS-protein interaction

We propose that each acylation influences the activation energy, and thus the rate of denaturation of the rungs of charge ladders of BCA in four ways (see schematic diagram in Fig. 1).

- i. Intermolecular electrostatic interaction. Each acylation increases the electrostatic repulsion between the more negatively charged proteins and the negatively charged SDS relative to the electrostatic repulsion between BCA and SDS. The increased electrostatic interaction increases the stability (and therefore,  $\Delta G^\ddagger$ ) of the latter rungs of the charge ladder, relative to unmodified BCA, to denaturation by SDS.

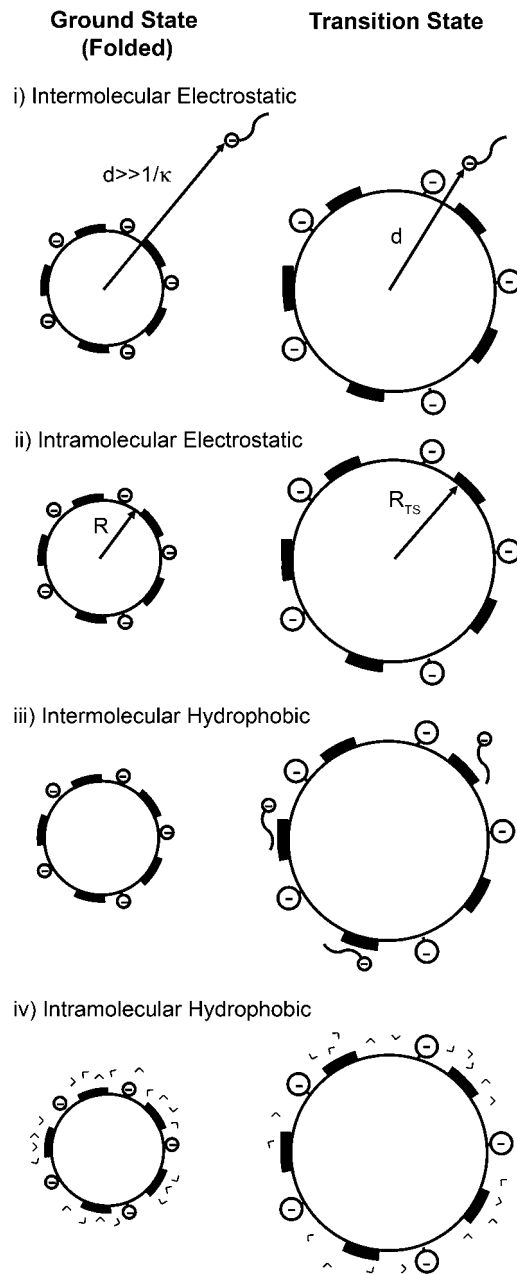


FIGURE 1 Schematic representation of the four factors discussed in the text for the model of protein denaturation. The protein is represented as a sphere with uniformly distributed negative charge on its surface. The dark patches represent hydrophobic regions on the surface of the protein that result from acylations. The depictions of SDS molecules are wavy lines (dodecanoic chain) with negatively charged headgroups (sulfate group). V-shaped entities represent water molecules.

- ii. Intramolecular electrostatic interaction. Each acylation decreases the stability of the folded protein, relative to BCA, by increasing the net charge on its surface. The charge-charge repulsion destabilizes the folded state of a protein relative to BCA and makes the latter rungs of the charge ladder less stable than the early rungs to denaturation by SDS. The intramolecular electrostatic

repulsion decreases  $\Delta G^\ddagger$  of each rung of the charge ladder relative to  $\Delta G^\ddagger$  of BCA.

- iii. Intermolecular hydrophobic interaction. Each acylation also increases the exposed hydrophobic surface area and destabilizes the folded protein relative to BCA due to an increase in the interaction between the protein and the hydrophobic tails of the SDS molecules.
- iv. Intramolecular hydrophobic interaction. Each acylation destabilizes the folded protein relative to BCA due to an increase in exposed hydrophobic surface area and an increased ordering of water in the folded state relative to unmodified BCA. Both of the effects of increased hydrophobic surface area (effects iii and iv) should make the latter rungs of the charge ladder less stable than the early rungs to denaturation with SDS.

This model does not account for any specific (local) interactions that are created or destroyed by acylation (e.g., removal of salt bridges between lysine and other anionic residues on the protein, steric interactions caused by increasing the size of the lysine residue, or specific interactions between positively charged residues and molecules of SDS); it treats the protein as a distribution of charges and hydrophobic surface area. A number of groups (67–69) have proposed that positively charged residues on the surface of the protein provide places for the negatively charged SDS molecules to bind and nucleate further unfolding. We neglect any such site-specific nucleation process in our model. Although neglecting local interactions runs the risk of neglecting important specific interactions, we demonstrate that our model replicates the trends in the data without using them. There is thus no need, at least for BCA, to consider local interactions to describe how the rate of denaturation changes with acylation of lysine residues.

We wished to quantify the relative importance of these stabilizing (electrostatic) and destabilizing (hydrophobic and electrostatic) effects as the number of modifications increased. In comparing rungs with the same number of modifications,  $n$ , across charge ladders made with different anhydrides, the charge remains the same, but the hydrophobicity differs. We assume that the patterns and regioselectivity of acylation with acetyl and hexanoyl ladders are similar. Thus, we can distinguish the effects of charge and hydrophobicity in one experimental system.

## EXPERIMENTAL PROCEDURES

### Sources of chemicals and reagents

All chemicals were reagent grade unless stated otherwise. Acetic anhydride, hexanoic anhydride, bovine carbonic anhydrase,  $10\times$  Tris-Gly concentrate, HEPBS, dioxane, and dimethylformamide were purchased from Sigma Chemical (Milwaukee, WI). Dialysis cassettes (weight cutoff of 10 kDa) and desalting spin columns were purchased from Pierce (Rockford, IL). SDS (Baker Chemical, Phillipsburg, NJ) was recrystallized in hot ethanol three times, then dried and stored at  $-20^\circ\text{C}$  until use. SDS was discarded or

repurified after 2 months. Tris-Gly buffer was made by diluting 100 mL of the 10× concentrate with 900 mL of freshly distilled, deionized water and filtered with a 0.22- $\mu\text{m}$  filter (Pall, Ann Arbor, MI) before use.

## Protein modification using hydrophobic anhydrides

We made solutions of 100  $\mu\text{M}$  of BCA in 500  $\mu\text{L}$  of 0.1M HEPBS buffer, pH 9. Stock solutions of anhydrides were made by diluting 10  $\mu\text{L}$  of anhydride (acetic or hexanoic) into 500  $\mu\text{L}$  dioxane. This stock solution was then diluted with dioxane to make concentrations of anhydride that were 6, 12, and 18 times the concentration of lysines (1.9 mM) in the reaction mixture. These reagents were made immediately before they were used. Twenty-five  $\mu\text{L}$  of each of the diluted stocks of anhydride were added to the protein solutions, so that the final ratio of anhydride to lysine was 0.3, 0.6, and 0.9 in each of the reaction mixtures. The mixtures were agitated immediately using a vortex mixer. The reactions were left overnight to ensure complete reaction. The proteins were desalted into 1× Tris-Gly buffer using spin desalting columns. Each reaction mixture was then run on CE to determine the relative concentration of each rung. The reaction mixtures were then combined so that the final concentration of each rung was approximately constant across the ladder.

## Denaturation experiments

A charge ladder of BCA (BCA-Ac<sub>n</sub> or BCA-Hex<sub>n</sub>, 1 mL of 100  $\mu\text{M}$  total protein in Tris-Gly buffer) was placed in a dialysis cassette (MW cutoff of 10 kDa). The dialysis cassette was placed in a 1 L bath of 3 mM SDS in Tris-Gly buffer at room temperature. The buffer was changed every 24 h. At regular intervals of time (approximately every half-hour), 100  $\mu\text{L}$  of the protein solution was removed from the dialysis cassette;  $\sim 7$   $\mu\text{L}$  of that aliquot was diluted 10-fold and the absorbance of the diluted sample at 280 nm ( $\epsilon_{280, \text{BCA}} = 57,000 \text{ M}^{-1}\text{cm}^{-1}$ , we assume that the absorption cross section is unchanged by acylation) was measured to determine the total protein concentration. We diluted the aliquot because the absorbance of the 100  $\mu\text{M}$  solution was too high to be read accurately by the ultraviolet spectrometer. This diluted aliquot was discarded. The remainder of the solution was then run on CE. The protein solution, except for the portion diluted for ultraviolet measurement, was returned to the dialysis cassette; the aliquot was outside of the dialysis cassette for  $\sim 5$  min.

## Capillary electrophoresis conditions

Capillary electrophoresis experiments were carried out in a Beckman (Fullerton, CA) PACE-MDQ system, using a capillary of inner diameter of 50  $\mu\text{m}$  of total length of 110.2 cm, 100 cm to the detector. Tris-Gly in D<sub>2</sub>O was used as the running buffer, and the applied voltage was 30 kV. D<sub>2</sub>O was used in place of H<sub>2</sub>O for the electrophoresis buffer because the viscosity of D<sub>2</sub>O is higher than that of H<sub>2</sub>O and the higher viscosity minimizes diffusion. Samples were injected using pressure (20 psi) for 30 s. Each sample contained 0.65 mM dimethylformamide as an electrically neutral marker for electroosmotic flow.

## RESULTS AND DISCUSSION

### Experimental protocol

The cmc of SDS in the Tris-Gly buffer used in this study is 4.3 mM (50). We chose 3 mM SDS for our studies of denaturation because this concentration of SDS denatures BCA in an interval of time that is convenient for experimental work using CE. In addition, this concentration of SDS is

close to the concentration often used in SDS-PAGE (0.1% or  $\sim 3.5$  mM) (1). We put 1 mL of a solution of  $\sim 100$   $\mu\text{M}$  of a charge ladder of BCA, dissolved in Tris-Gly buffer, into a dialysis cassette (molecular weight cutoff of 10 kDa) and placed the cassette in 1 L of Tris-Gly buffer containing 3 mM SDS. The bath was kept at room temperature ( $\sim 22^\circ\text{C}$ ) for the duration of the experiment.

SDS molecules pass through the dialysis cassette, but the protein and protein-SDS aggregates and SDS micelles do not. We used the dialysis cassette because we wanted to maintain a constant concentration of free SDS in the solution around the protein. If we assume that BCA and its charge variants, like most proteins, bind SDS at a ratio of  $\sim 1$  SDS molecule per 2 amino acids (8–11), each BCA molecule should bind  $\sim 130$  SDS molecules. Because BCA binds so many molecules of SDS, it is difficult to keep the concentration of free SDS constant without a large source (here using a dialysis cassette). Without a dialysis cassette, we would be constrained to study denaturation at concentrations of SDS more than 130 times the protein concentration (100  $\mu\text{M}$  in these experiments) i.e., above 13 mM. With the dialysis cassette, we are able to add molecules of SDS to the system without changing the concentration of free SDS, and to study the denaturation of proteins below the cmc of SDS. (We attempted to measure the relative rates of denaturation of rungs of BCA-Ac<sub>n</sub> using buffer containing 10 mM SDS, but the proteins denatured in the time it takes to measure the electropherograms. The experiment, as designed, cannot be done above the cmc because the time it takes to denature some rungs becomes faster than the time of a CE run.)

At regular intervals of time (approximately every half hour), we removed 100- $\mu\text{L}$  aliquots of the solutions containing the charge ladder of BCA from the cassette in a bath of 3 mM SDS in Tris-Gly buffer, measured the total protein concentration in the aliquot using absorbance at 280 nm, and injected a portion ( $\sim 10$  nL) of the aliquot onto the CE. The unused portions of the aliquots were then returned to the cassette. The aliquots were out of the dialysis cassette for  $< 5$  min; this time is shorter than the shortest times for denaturation ( $\sim 16$  min) measured in our experiments for denaturation, and therefore should not significantly affect our measurements.

### Corrections of peak areas

Fig. 2 shows electropherograms as a function of time for the acetyl- and hexanoyl charge ladders of BCA. To quantify the rate of denaturation of each rung of the charge ladders, the peaks were integrated and then corrected for three factors.

#### *Residence time in the detection volume*

Proteins that have a higher velocity along the capillary spend less time in the detection volume than proteins that have lower velocity. If two proteins with the same absorptivity

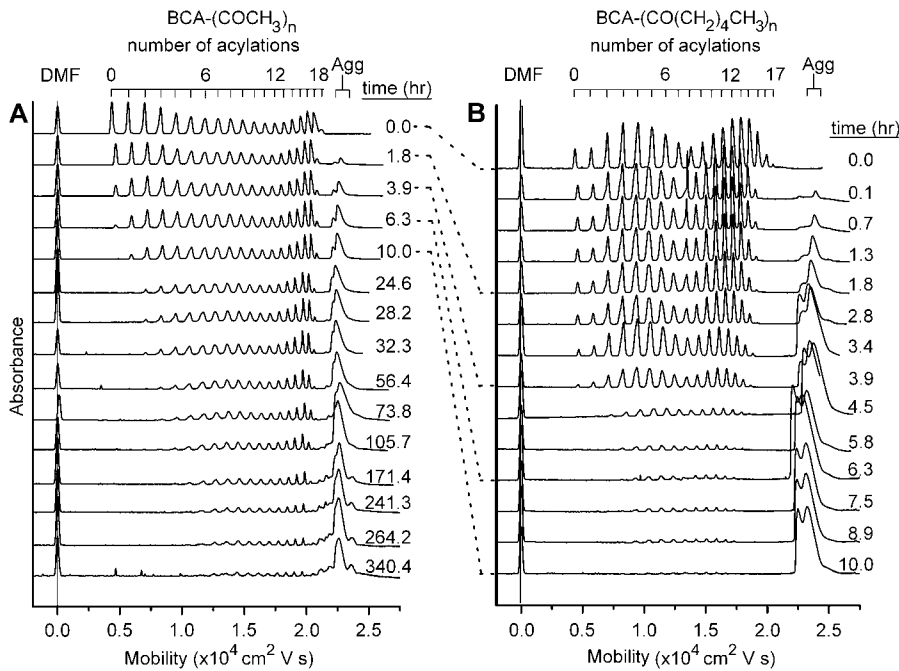


FIGURE 2 Denaturation of hydrophobic charge ladders of (A) BCA-Ac<sub>n</sub> and (B) BCA-Hex<sub>n</sub>. Dimethylformamide was used as a neutral marker of electroosmotic flow. Each ladder is labeled with the time elapsed after placing the dialysis cassette containing protein in the solution of SDS; the dotted lines match up measurements of BCA-Ac<sub>n</sub> and BCA-Hex<sub>n</sub> measured at the same amount of elapsed time. The peak corresponding to denatured, aggregated BCA-SDS is labeled (Agg) and has fine structure; this structure may be due to different denatured states of the BCA-SDS aggregate.

were present in a sample in equal concentrations, the protein of lower velocity would have a larger measured peak area than the protein of higher velocity. To correct for this experimental bias, we multiplied the area of each peak by the velocity of the protein ( $A_{\text{corr}} = A_{\text{measured}} \times L_D/t_D$ ), where  $L_D$  is the length of the capillary from the end (where injection occurs) to the detector (100 cm in all of our experiments) and  $t_D$  is the time it takes for the rung to reach the detector (71).

#### Initial differences in concentrations of each rung

The areas of each of the rungs in the charge ladder were not all equal before denaturation. To measure the fraction of each rung that has denatured at each time, the velocity-corrected area of each rung in the sample was divided by the velocity-corrected area of that rung in the charge ladder run in the absence of SDS.

#### Loss of protein due to dialysis

The total protein concentration, as measured by absorbance at 280 nm, decreased by ~15% over a week of dialysis, presumably through association with the dialysis membrane, and/or leakage out of the dialysis cassette. The correction for total protein concentration assumes that regardless of the mechanism by which protein is lost, each rung is lost equally.

#### Comparison of the rates of denaturation

Fig. 3 shows the decrease in corrected peak area as a function of time for representative rungs of the BCA-Ac<sub>n</sub> and BCA-Hex<sub>n</sub> charge ladders. We fit each of these sets of data to a

single exponential decay and plotted the rate of denaturation as a function of rung number (Fig. 4 A). In principle, since every rung (except the native—BCA—and fully functionalized proteins—BCA-Ac<sub>18</sub>) is a collection of regioisomers, the denaturation profile may not be a single exponential function. We use the single exponential as a measure of the relative rates of denaturation of each rung. The exact functional form is not required for our analysis, and each set of the data in Fig. 3 appears to fit a single exponential well. Fig. 4 A shows that there is a pronounced minimum in the plot of the rates of denaturation versus number of acylations for both charge ladders; the earlier and later rungs denature more rapidly, and the middle rungs denature least rapidly.

#### Mathematical model of the kinetics of the interaction of charge ladders of BCA with SDS

As we described in the introduction, we propose a model in which there are two types of interactions—electrostatic and hydrophobic—that change the  $\Delta G^\ddagger$  for denaturation of modified BCA by SDS relative to that of BCA. Each of the two types of interactions has an intermolecular component that describes how the modification changes the interaction between SDS and protein, and an intramolecular component that describes how the modification changes the stability of the modified BCA in the absence of SDS. Here we will construct a mathematical description of the model to fit the data describing rate of denaturation versus the number of acylations (Fig. 4 A).

The four types of interactions should add to give the total activation energy of denaturation for each rung of a charge ladder (Eq. 2), where  $\Delta G_{\text{BCA-X}_n}^\ddagger$  is the activation

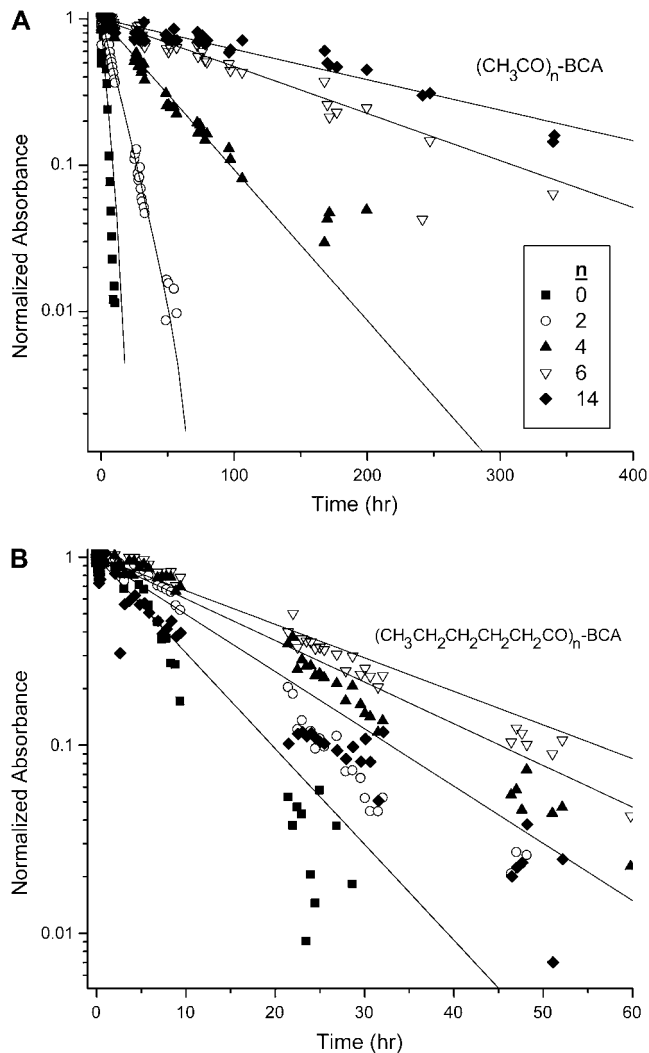


FIGURE 3 Corrected areas (see text for details) as a function of time for representative rungs of (A) an  $\text{BCA-Ac}_n$  charge ladder and (B) a  $\text{BCA-Hex}_n$  charge ladder. Deviations from linearity could be due to the fact that each rung of the charge ladder is made up of a mixture of regioisomers that may have different rates of denaturation. The data shown in this figure are from one experiment. (It is difficult to give experimental uncertainties to the points on the graph because the time at which the points were taken differed between repetitions of the experiment.)

$$\Delta G_{\text{BCA-Xn}}^{\ddagger} = \Delta G_{\text{BCA}}^{\ddagger} + \Delta \Delta G_{\text{e-p,SDS}}^{\ddagger} + \Delta \Delta G_{\text{e-p}}^{\ddagger} + \Delta \Delta G_{\text{hydro,p,SDS}}^{\ddagger} + \Delta \Delta G_{\text{hydro,p}}^{\ddagger} \quad (2)$$

energy of denaturation for the  $n$ th rung of a charge ladder,  $\Delta G_{\text{BCA}}^{\ddagger}$  is the activation energy of unmodified BCA, and the other terms are the additional activation energies of unfolding, relative to BCA, due to i), intermolecular electrostatic repulsion between the SDS molecule and the modified BCA ( $\Delta \Delta G_{\text{e-p,SDS}}^{\ddagger}$ ); ii), intramolecular electrostatic repulsion between the charges on the surface of the modified BCA ( $\Delta \Delta G_{\text{e-p}}^{\ddagger}$ ); iii), intermolecular hydrophobic interaction between the SDS molecules and modified BCA ( $\Delta \Delta G_{\text{hydro,p,SDS}}^{\ddagger}$ ); and iv), intramolecular hydrophobic interaction due to the

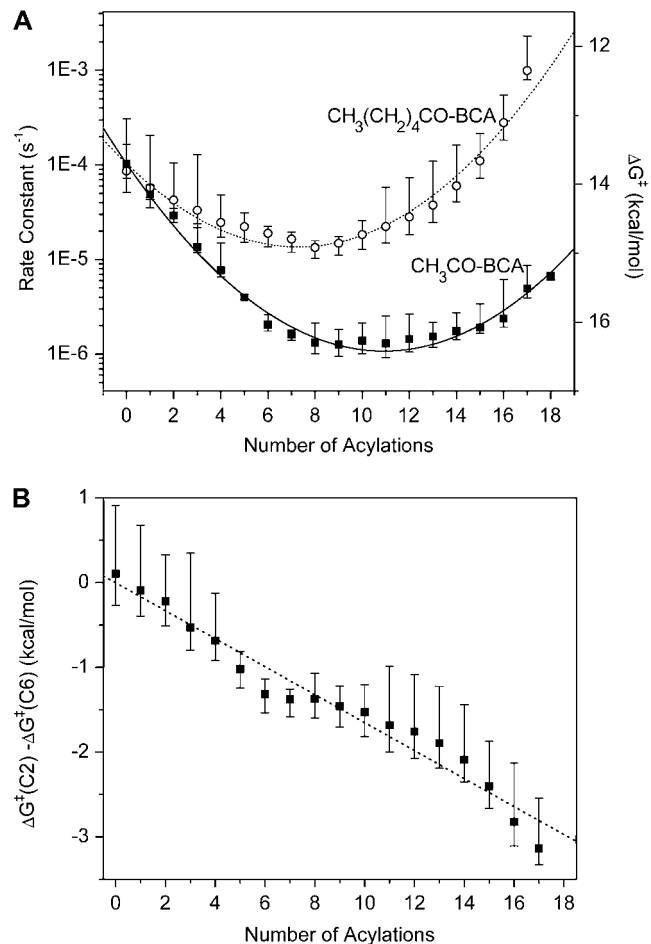


FIGURE 4 (A) Rate constants of denaturation for both (■)  $\text{BCA-Ac}_n$  and (○)  $\text{BCA-Hex}_n$  charge ladders with SDS as a function of the number of acylations. The points are the arithmetic average and the error bars are minimum and maximum values measured in three repetitions for  $\text{BCA-Ac}_n$  and four repetitions for  $\text{BCA-Hex}_n$ . The right y axis shows the corresponding  $\Delta G^{\ddagger}$  in kcal/mol calculated using Eq. 1. The lines show fits of the equation  $\Delta G^{\ddagger} = a + bn + cn^2$  to the data; see text for discussion of this model. (B) A plot of the difference in  $\Delta G^{\ddagger}$  between a rung of an acetyl ladder and a hexanoyl ladder as a function of rung number. The data fit a line (slope = 0.17 kcal/mol,  $R^2 = 0.97$ ). The fit of these data to a linear plot (dotted lines) suggests that the difference in  $\Delta G^{\ddagger}$  between the two ladders is only due to the difference in the linear term  $bn$ ; the  $c$  coefficient includes only electrostatic contributions to  $\Delta G^{\ddagger}$ .

additional exposed hydrophobic residues on the surface of modified BCA ( $\Delta \Delta G_{\text{hydro,p}}^{\ddagger}$ ). To write down a functional form for each of these interactions, and to build a tractable model, we must apply a number of approximations to simplify the system composed of the protein, surfactant, and aqueous solvent.

### Assumptions in the mathematical description of the model

We approximate both the structure of the folded protein and the structure of the transition state as spheres with net charge uniformly distributed on the surface, and with a uniform

dielectric constant inside this shell of charge. The model we propose ignores all molecular-level details of protein, surfactant, and the solvent. The number (and distribution) of the molecules of SDS that bind to the protein in the transition state are also considered to be constant for all rungs of the charge ladders. This assumption concerning the stoichiometry of the transition state is suspect, but required to write an equation for the intermolecular electrostatic repulsion term; we assume a single value for the number of SDS molecules bound in the transition state ( $m$ ) for all BCA derivatives. We assume the value of dielectric constant of water ( $\epsilon_w$ ) is 80, and we neglect the change in the dielectric constant that probably occurs near the surface of the protein. Others have shown that the dielectric constant of water is close to 20 over a few layers of water molecules (a few angstroms) due to the reduced mobility of the water molecules next to the surface of the protein (72). The dielectric constant is probably affected by the distribution of charged, polar, and apolar groups in the protein and the net charge of the protein (56). We further assume that the dielectric constant is uniform throughout the interior of the protein ( $\epsilon_p = 5$ ) (72). In real systems, the dielectric constant is structured on a microscopic scale and may vary with position. The dielectric constant of solvent-exposed regions of the protein is probably higher than the interior due to configurational mobility of polar side chains (73).

Each conversion of a lysine- $\epsilon$ -NH<sub>3</sub><sup>+</sup> group to a lysine- $\epsilon$ -NHCOR group changes the charge ( $\Delta Z$ ) by <1 unit of charge, reflecting charge regulation (54,55). The value of  $\Delta Z$  is close to  $-0.9$  for the first few acylations in the conditions we used (pH 8.4), and is probably  $<-0.9$  (probably between  $-0.7$  and  $-0.9$ ) at high numbers of acylation. We will assume that  $\Delta Z = -0.9$  for all acylations regardless of the acylating reagent and number of prior acylations (that is, for example, we assume that BCA-Ac<sub>5</sub> and BCA-Hex<sub>5</sub> have the same net charge and charge distribution). In these calculations, we consider only first-order electrostatic interactions. We will ignore any higher-order electrostatic interactions (for example, charge-dipole and charge-induced dipole effects) between the charged surfactant and protein (assumed to be a dielectric sphere).

This model is clearly a draconian simplification, relative to the real proteins. Proteins are not a spherical shell of charges—not all of the charges are uniformly distributed or located at the surface of the protein, and the protein can compensate for additional charges by changing the values of pK<sub>a</sub> of nearby groups (54,55). Using these assumptions, we can, however, derive equations for each of the terms in Eq. 2.

### Intermolecular electrostatic repulsion between SDS and BCA

The repulsion between a negatively charged molecule of SDS and a protein can be described by Coulomb's law in

water containing salts (Eq. 3), where  $q_{\text{SDS}}$  is the charge on SDS ( $-1 e_c$ ),  $e_c$  is the charge of

$$E = \frac{q_{\text{SDS}}q_{\text{BCA-X}_n}}{4\pi\epsilon_0\epsilon_w d(1 + \kappa d)} \quad (3)$$

an electron,  $q_{\text{BCA-X}_n}$  is the charge on the  $n$ th rung of the charge ladder,  $\epsilon_w$  is the dielectric constant of water,  $\epsilon_0$  is the permittivity of free space,  $d$  is the distance between the center of the sphere representing the protein and the molecule of SDS, and  $\kappa$  is the inverse Debye length ( $0.333 \text{ nm}^{-1}$  in Tris-Gly buffer, ionic strength of 10 mM). The  $\Delta\Delta G_{e-p,\text{SDS}}^\ddagger$  term (the difference between  $\Delta G_{e-p,\text{SDS}}^\ddagger$  for BCA-X<sub>n</sub> and for BCA) is then given by Eq. 4 where  $q_{\text{BCA}}$  is the charge on

$$\begin{aligned} \Delta\Delta G_{e-p,\text{SDS}}^\ddagger &= \Delta\Delta G_{e-p,\text{SDS}}^\ddagger(\text{BCA} - \text{X}_n) - \Delta\Delta G_{e-p,\text{SDS}}^\ddagger(\text{BCA}) \\ &= \frac{mq_{\text{SDS}}q_{\text{BCA-X}_n}}{4\pi\epsilon_0\epsilon_w d(1 + \kappa d)} - \frac{mq_{\text{SDS}}q_{\text{BCA}}}{4\pi\epsilon_0\epsilon_w d(1 + \kappa d)} \\ &= \frac{-me_c^2\Delta Zn}{4\pi\epsilon_0\epsilon_w d(1 + \kappa d)} \end{aligned} \quad (4)$$

native BCA ( $Z_0 = -3 e_c$ ), and  $m$  is the number of molecules of SDS that are bound to the protein in the transition state.

We consider only values of free energy in this calculation. In water, the relative partitioning of the free energy due to Coulombic interactions into enthalpy and entropy is complicated, and the majority of the free energy may be due to entropy (not due to enthalpy—the major portion of the free energy in vacuum) (56). In the interaction of protein with molecules of SDS, it is unclear whether the solvation (entropic effects) or enthalpy is the primary contributor to  $\Delta G$ .

### Intramolecular charge/charge repulsion

The change in energy upon adding a charge to a uniform shell of charge on the surface of a protein is given by Eq. 5, where

$$\begin{aligned} \Delta\Delta G_{e-p}^\ddagger &= \frac{q_{\text{BCA-X}_n}^2 - q_{\text{BCA}}^2}{8\pi\epsilon_0\epsilon_p R(1 + \kappa R)} - \frac{q_{\text{BCA-X}_n}^2 - q_{\text{BCA}}^2}{8\pi\epsilon_0\epsilon_p R_{\text{TS}}(1 + \kappa R_{\text{TS}})} \\ &= \frac{e_c^2(Z_0 - n\Delta Z)^2 - e_c^2 Z_0^2}{8\pi\epsilon_0\epsilon_p R(1 + \kappa R)} - \frac{e_c^2(Z_0 - n\Delta Z)^2 - e_c^2 Z_0^2}{8\pi\epsilon_0\epsilon_p R_{\text{TS}}(1 + \kappa R_{\text{TS}})} \\ &= \frac{e_c^2}{8\pi\epsilon_0\epsilon_p} \left( \frac{1}{R(1 + \kappa R)} - \frac{1}{R_{\text{TS}}(1 + \kappa R_{\text{TS}})} \right) \\ &\quad \times (-2Z_0\Delta Zn + n^2). \end{aligned} \quad (5)$$

$R$  is the radius of the protein,  $\epsilon_p$  is the dielectric constant in the interior of the protein, and  $R_{\text{TS}}$  is the radius of the transition state. This equation approximates both the folded protein and the transition state of the protein-SDS aggregate as spheres.



Because we have assumed that  $\Delta Z$  is the same for acylations in all positions, and because we have assumed that the charge is uniformly distributed on the surfaces of the spherical protein, proteins contained in a given rung of the charge ladder, even though they are regioisomers, should repel a molecule of SDS with the same force. The two equations (3 and 5) that describe how changes in electrostatics affect changes to  $\Delta G^\ddagger$  will, therefore, be the same for both the acetyl and hexanoyl charge ladders.

### Hydrophobic contributions to $\Delta G^\ddagger$

#### *Intermolecular hydrophobic interaction between exposed hydrophobic surface area of BCA and molecules of SDS*

The additional exposed hydrophobic surface area on the acylated proteins relative to BCA increases the interaction (and hence the equilibrium constant for association) between SDS molecules and the protein. We assume that this increase in interaction is proportional to the additional hydrophobic surface area of the acylated proteins relative to unacylated BCA (Eq. 6); in this equation  $n$  is the number of modifications and

$$\Delta\Delta G_{\text{hydro,p-SDS}}^\ddagger = C_{\text{hydro,p-SDS}} \cdot n. \quad (6)$$

$C_{\text{hydro,p-SDS}}$  is a constant of proportionality that is larger for hexanoyl than for acetyl ladders. The ratio of the  $\pi$ -parameters described in the introduction suggests that each modification with hexanoic anhydride results in a change in hydrophobicity that is similar to three acylations with acetic anhydride, and therefore, that  $C_{\text{hydro,p-SDS}}(\text{BCA-Hex}_n) \cong 3 C_{\text{hydro,p-SDS}}(\text{BCA-Ac}_n)$ .

#### *Intramolecular destabilization due to additional exposed hydrophobic surface area*

The increase in the exposed hydrophobic area on the surface of the acylated BCA relative to BCA should also decrease the stability of the folded protein. The increase in exposed surface area increases the order of the water surrounding the protein, thereby decreasing the entropy in the folded state. The increase in ordered water molecules around hydrophobic residues relative to BCA should be greatest in the folded state; in the denatured state, there is a large exposed surface, and the change due to the chemical modification of lysine residues should be minimal. The  $\Delta\Delta G_{\text{folding}}^\circ$  between acylated BCA and BCA is, then, primarily due to a destabilization of the ground state; this destabilization should also affect  $\Delta\Delta G^\ddagger$  because the transition state should be less affected than the folded state. (The configurational entropy of the modified side chains in the native and transition states may also contribute to the stability of the derivatives. The relative configurational entropy in the ground and the transition state could also increase the rate of denaturation of modified BCA relative to native BCA.)

The free energy required to transfer a hydrocarbon from the pure hydrocarbon phase to water is a linear function of the surface area of the chain (75,76). Zhou and Zhou have generated an empirical stability scale for hydrophobic residues using 1023 point mutations to 35 different proteins (77). They demonstrated that a change in hydrophobic surface area on a protein contributes  $12\text{--}28 \text{ cal mol}^{-1} \text{ \AA}^{-2}$  to  $\Delta G_{\text{unfolding}}^\circ$ . Using the stability scale measured by Zhou and Zhou as justification, we assume that the difference in free energy of folding between acylated BCA and BCA ( $\Delta\Delta G_{\text{folding}}^\circ$ ), and also the destabilization of the folded state relative to the transition state ( $\Delta\Delta G^\ddagger$ ), is linear with the number of acylations (Eq. 7); where  $C_{\text{hydro,p}}$  is a

$$\Delta\Delta G_{\text{hydro,p}}^\ddagger = C_{\text{hydro,p}} \cdot n \quad (7)$$

constant of proportionality that differs between charge ladders and should be proportional to size of the surface area of the acylating reagent used. Because hexanoyl groups are  $\sim 3$  times the surface area of acetyl group,  $C_{\text{hydro,p}}(\text{BCA-Hex}_n) = 3 C_{\text{hydro,p}}(\text{BCA-Ac}_n)$ .

We also performed a surface area calculation to determine the change in surface area between the conversion of BCA to  $\text{BCA-Ac}_{18}$  and BCA to  $\text{BCA-Hex}_{18}$ . We calculated that the reaction with acetic anhydride changed the surface area of BCA by  $400 \text{ \AA}^2$  and the reaction with hexanoic anhydride changed the surface area of BCA by  $1180 \text{ \AA}^2$ . Since this change is a factor of 2.9, we conclude that our estimate that each modification with hexanoic anhydride adds three times the amount of surface area than modification with acetic anhydride is justified.

#### *Treatment of the changes to hydrophobicity in the model*

Because  $\Delta\Delta G_{\text{hydro,p-SDS}}^\ddagger$  and  $\Delta\Delta G_{\text{hydro,p}}^\ddagger$  have the same functional form within our model, the same dependence on the number of modifications, and the same dependence on the identity of the anhydride ( $3 \cdot C_{\text{hydro}}(\text{Ac}) = C_{\text{hydro}}(\text{Hex})$ ), we will not be able to distinguish between the intermolecular and intramolecular effects of changes in hydrophobicity. We will only be able to measure the cumulative  $\Delta\Delta G_{\text{hydro}}^\ddagger$  (Eq. 8). Here,  $C_{\text{hydro}}$  is a proportionality constant and is equal to  $C_{\text{hydro,p-SDS}} + C_{\text{hydro,p}}$ :

$$\Delta\Delta G_{\text{hydro}}^\ddagger = \Delta\Delta G_{\text{hydro,p-SDS}}^\ddagger + \Delta\Delta G_{\text{hydro,p}}^\ddagger = C_{\text{hydro}} \cdot n \quad (8)$$

#### *Combination of electrostatic and hydrophobic terms into a single equation*

By substituting Eqs. 3, 4, and 8 into Eq. 2, we can express the activation energy of each rung of the charge ladder as a function of the number of acylations,  $n$  (Eq. 9). The non-linear term in Eq. 9 only depends on intramolecular electrostatic repulsion. Since the data

$$\Delta G_{\text{BCA}-X_n}^{\ddagger} = \Delta G_{\text{BCA}}^{\ddagger} + \frac{m e_c^2 \Delta Z n}{4 \pi \epsilon_0 \epsilon_w d (1 + \kappa d)} - \frac{e_c^2}{8 \pi \epsilon_0 \epsilon_p} \left( \frac{1}{R(1 + \kappa R)} - \frac{1}{R_{\text{TS}}(1 + \kappa R_{\text{TS}})} \right) \times (-2 Z_0 \Delta Z n + n^2) - C_{\text{hydro}} n \quad (9)$$

in Fig. 4 A are clearly nonlinear, we can conclude that the intramolecular electrostatic repulsion is an important factor in the denaturation of proteins, especially when the net charge on the protein becomes large ( $>10 e_c$  for BCA). Since this repulsion depends only on parameters of the protein (and not the SDS molecules), it may play a role in protein stability and denaturation with other denaturants.

There are four unknown parameters ( $m$ , the number of molecules of SDS bound to the protein in the transition state,  $R_{\text{TS}}$ , the radius of the transition state,  $d$ , the distance between the SDS molecules and the protein in the transition state, and  $C_{\text{hydro}}$ , a constant representing the sum of the hydrophobic interactions) in Eq. 9; it is not possible to measure or estimate these parameters because they depend on the geometry of the transition state. We therefore estimate those parameters using our model and the data in Fig. 4 A, and decide if the calculated values for these parameters seem physically reasonable.

#### Analysis of the relative rates of denaturation of different rungs to the proposed model

The model predicts that a second-order polynomial describes the rate of denaturation as a function of the number of acylations. We fit the data in Fig. 4 A to a second-order polynomial ( $a + b n + c n^2$ ), where  $n$  is the number of acylations. The fits of the two charge ladders were constrained to obtain the best fit for both ladders, with  $a$  and  $c$  constrained to the same value for both ladders because they describe the electrostatic terms (which we assume to be invariant). Fig. 4 A shows the fits. (If the data for BCA-Ac<sub>n</sub> and BCA-Hex<sub>n</sub> are fit independently, the values for  $a$  and  $c$  for each data set are within error of each other.) The coefficients  $a$  and  $c$  are independent of the kind of acylation because they do not depend on the hydrophobicity of the reagent; they depend only on the electrostatic interactions. As a result, the difference in activation energies between acetyl and hexanoyl ladders (Eq. 10) should be linear (Fig. 4 A). The slope ( $-0.17$  kcal/mol of

$$\Delta \Delta G^{\ddagger} = \Delta G^{\ddagger}(\text{BCA} - \text{Ac}_n) - \Delta G^{\ddagger}(\text{BCA} - \text{Hex}_n) \quad (10)$$

protein) is equal to  $\Delta C_{\text{hydro}}$ , where  $\Delta C_{\text{hydro}} = C_{\text{hydro}}(\text{Ac}) - C_{\text{hydro}}(\text{Hex}) = C_{\text{hydro}}(\text{Ac}) - 3 C_{\text{hydro}}(\text{Ac}) = -2 C_{\text{hydro}}(\text{Ac})$ . Therefore,  $C_{\text{hydro}}(\text{Ac}) = 0.085$  kcal/mol and  $C_{\text{hydro}}(\text{Hex}) = 0.26$  kcal/mol per acylation.

We found that  $\Delta G^{\ddagger}$  for BCA (i.e., the  $a$  coefficient) was  $14 \pm 1$  kcal/mol; this value will be directly affected by our estimate that  $\nu \kappa_{\text{TST}} = 10^6 \text{ s}^{-1}$ . If we underestimated the value of  $\nu \kappa_{\text{TST}}$ , the actual  $\Delta G^{\ddagger}$  for BCA will be lower.

The  $c$  coefficient—due only to intramolecular electrostatic destabilization—was  $-0.023 \pm 0.001$  kcal/mol of protein. (The negative sign on the  $c$  coefficient indicates that the intramolecular electrostatic repulsion decreases  $\Delta G^{\ddagger}$ . The negative sign is expected because this repulsion should destabilize the folded state of the protein and decrease the magnitude of the activation energy of denaturation.) Using the model, and assuming a radius of BCA of 2 nm, we calculate  $R_{\text{TS}}$  to be 2.1 nm. This radius is 5% larger than that of the folded protein, and we speculate that the protein remains relatively compact in the transition state.

The  $b$  coefficient for BCA-Ac<sub>n</sub> was  $0.50 \pm 0.01$  kcal/mol of protein; the  $b$  coefficient for BCA-Hex<sub>n</sub> was  $0.33 \pm 0.01$  kcal/mol of protein. This parameter has four components (see Eq. 9): i), electrostatic repulsion between the protein and SDS molecules, ii), the linear portion of the intramolecular electrostatic term, iii), hydrophobic interaction between protein and SDS, and iv), destabilization of the protein due to exposed hydrophobic surface area. From the calculations above, we estimate that  $C_{\text{hydro}}(\text{acetyl}) = 0.085$  kcal/mol and  $C_{\text{hydro}}(\text{hexanoyl}) = 0.26$  kcal/mol, and that  $R_{\text{TS}} = 2.1$  nm. We then have two remaining unknown parameters,  $d$  and  $m$ , but only one equation to constrain them. We can, however, make reasonable assumptions about one of these parameters and see if the corresponding value for the other parameter is reasonable. If we assume  $d$  is the radius of the protein in the transition state (2.1 nm), we calculate a value for  $m$  of  $\sim 7$  molecules of SDS bound in the transition state. If we guess that  $m$  is  $\sim 10$  molecules of SDS, we calculate a value for  $d$  of 2.8 nm.

We know that  $d$  should not be much larger than the Debye length (3 nm in our buffer) or the interactions should be heavily screened. With the assumptions made in this highly simplified model, we conclude that there are  $\sim 10$  molecules of SDS bound in the transition state. Since this number is  $\sim 1$  order of magnitude lower than the  $\sim 130$  molecules of SDS bound to the protein when completely denatured, we conclude that there are a small number of SDS molecules that interact with the protein and cause changes to the conformation of the protein. The rest of the molecules of SDS thus bind to the denaturing protein in later, nonrate determining steps.

#### Interpretation of the results of the fitting

Fig. 5 shows a schematic diagram of how the four effects in the model affect the height of the activation barrier. It also shows a plot of the contributions of  $\Delta G_{\text{e-p,SDS}}^{\ddagger}$ ,  $\Delta G_{\text{e-p}}^{\ddagger}$ , and  $\Delta G_{\text{hydro}}^{\ddagger}$  to  $\Delta \Delta G^{\ddagger}$  between BCA and each rung of the charge ladder. For both BCA-Ac<sub>n</sub> and BCA-Hex<sub>n</sub>, net electrostatics contribute more to  $\Delta G^{\ddagger}$  than hydrophobicity. The contribution to  $\Delta \Delta G^{\ddagger}$  due to the changes in net charge of the protein is shown as the dotted red/green line. At low values of  $n$ , the  $\Delta G_{\text{e-p}}^{\ddagger}$  term dominates and the modified proteins have a higher activation energy than the native BCA. At high values of  $n$ , the contributions of  $\Delta G_{\text{e-p,SDS}}^{\ddagger}$  and  $\Delta G_{\text{e-p}}^{\ddagger}$  largely offset each other. For BCA-Hex<sub>n</sub>, the effects of changes in

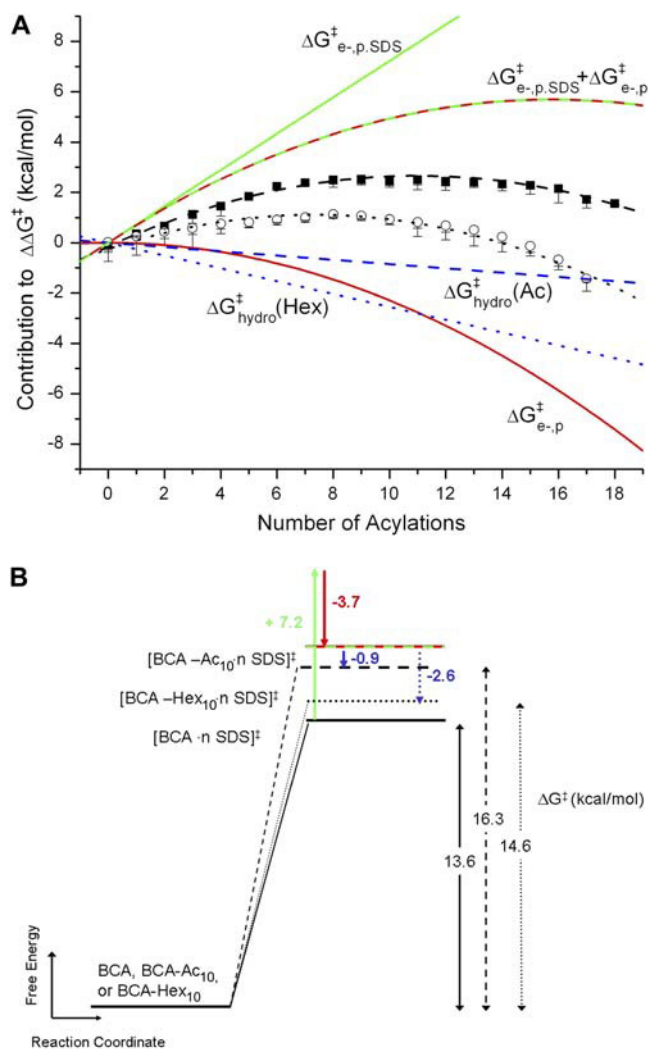


FIGURE 5 (A) Contributions to  $\Delta\Delta G^\ddagger$  from  $\Delta G_{e-p,SDS}^\ddagger$  (green line),  $\Delta G_{e-p}^\ddagger$  (red line), and  $\Delta G_{hydro}^\ddagger$  (blue line; dashed line, Ac<sub>n</sub>, and dotted line, Hex<sub>n</sub>). The sum of the electrostatic contributions is marked as the red-green dashed line. The data for  $\Delta\Delta G^\ddagger$ —the sum of the four components—are shown for BCA-Ac<sub>n</sub> (■) and BCA-Hex<sub>n</sub> (○). The fits to the data (dashed line, BCA-Ac<sub>n</sub>; dotted line, BCA-Hex<sub>n</sub>) are those given by Eq. 9. See text for details of the model. (B) An example of how the energy of the transition state changes relative to that of the ground state with 10 modifications. The folded states of BCA, BCA-Ac<sub>10</sub>, and BCA-Hex<sub>10</sub> are scaled to the same energy. The arrows (in the same colors as A) indicate how each of the factors changes the relative position of the transition state. The red/green dashed line shows the effects of just the electrostatic terms on the energy of the transition state (i.e., if 10 lysine groups were neutralized with no corresponding change in hydrophobicity).

hydrophobicity (dotted blue line) are nearly the same in magnitude as the effects of changes in electrostatics.

The data are consistent with the model presented, but the good agreement between the model and the data are certainly not proof that this model is an accurate description of the molecular processes involved in denaturation. The assumptions discussed earlier are simplifications of a complex biochemical system, and the simplistic model can only begin

to identify free energies that may be important in determining how the stability of a protein is changed by chemical modifications to that protein and how surfactants denature proteins. Nonetheless, the model described here offers a first step toward understanding the major components of a very complicated and poorly understood system.

## CONCLUSIONS

Hydrophobic charge ladders are a useful tool for determining the relative importance of charge and hydrophobicity in the denaturation of proteins with SDS. Charge ladders provide data in which charge and hydrophobicity vary independently. These data allow us to estimate quantitatively the relative importance of electrostatics and hydrophobicity in the rate of denaturation of BCA (and, in principle, other proteins) with SDS. In particular, the study with acetyl and hexanoyl charge ladders of BCA indicates that both charge and hydrophobicity affect the rate of denaturation of BCA with SDS. We conclude that the effects of charge on denaturation with SDS are ~5-fold larger than the effects of hydrophobicity for BCA-Ac<sub>n</sub> and of similar size for BCA-Hex<sub>n</sub>.

To account for the curvature in the data of rate of denaturation versus number of acylations, we must include a nonlinear term that describes intramolecular electrostatic repulsion. The functional form of the model described in this study fits well to the data for BCA-Ac<sub>n</sub> and BCA-Hex<sub>n</sub>; we conclude that the four terms included in our model—inter- and intramolecular electrostatic repulsion, and inter- and intramolecular hydrophobic interactions—give a plausible description of the major factors in determining the change in the rate of denaturation with acylation. Results suggest that removing small amounts of negative charge (~1–10  $e_c$ ) from the surface of a protein may stabilize that protein to denaturation with SDS, but that removing large amounts of charge (>15  $e_c$ ) will destabilize the protein. There is, therefore, an optimum amount of surface charge to make a protein stable to SDS denaturation and, at least for one protein (BCA), this ideal charge is different from that of the native protein. The strength of using charge ladders is that the effects are averaged over multiple species (regioisomers). The fact that we can describe the denaturation of the set of them represented by each rung of the ladder with a simple, intuitive model, and a common set of numerical constants, implies that the rate of denaturation is dominated by global (nonlocal) effects.

## SUPPLEMENTARY MATERIAL

An online supplement to this article can be found by visiting BJ Online at <http://www.biophysj.org>.

We acknowledge Logan McCarthy, Hongkai Wu, and Chengde Mao for helpful discussions and the National Institutes of Health for research support (GM51559).

## REFERENCES

- Gallagher, S. R. 2005. One-dimensional SDS gel electrophoresis of proteins. *In* Current Protocols in Molecular Biology. F. M. Ausubel, R. Brent, R. E. Kingston, D. D. Moore, J. G. Seidman, J. A. Smith, and K. Struhl, editors. John Wiley & Sons, New York. 10.2A.1–10.2A.34.
- Rigaud, J. L., M. Chami, O. Lambert, D. Levy, and J. L. Ranck. 2000. Use of detergents in two-dimensional crystallization of membrane proteins. *Biochim. Biophys. Acta.* 1508:112–128.
- le Maire, M., P. Champeil, and J. V. Moller. 2000. Interaction of membrane proteins and lipids with solubilizing detergents. *Biochim. Biophys. Acta.* 1508:86–111.
- Jones, M. N. 1999. Surfactants in membrane solubilisation. *Int. J. Pharm.* 177:137–159.
- Svenson, S. 2004. Controlling surfactant self-assembly. *Curr. Opin. Colloid Interface Sci.* 9:201–212.
- Duro, R., C. Souto, J. L. Gomez-Amoza, R. Martinez-Pacheco, and A. Concheiro. 1999. Interfacial adsorption of polymers and surfactants: implications for the properties of disperse systems of pharmaceutical interest. *Drug Dev. Ind. Pharm.* 25:817–829.
- Jones, L. S., N. B. Bam, and T. W. Randolph. 1997. Surfactant-stabilized protein formulations: a review of protein-surfactant interactions and novel analytical methodologies. *ACS Symp. Ser.* 675:206–222.
- Pitt-Rivers, R., and F. S. A. Impiombato. 1968. Binding of sodium dodecyl sulfate to various proteins. *Biochem. J.* 109:825–830.
- Fish, W. W., J. A. Reynolds, and C. Tanford. 1970. Gel chromatography of proteins in denaturing solvents. Comparison between sodium dodecyl sulfate and guanidine hydrochloride as denaturants. *J. Biol. Chem.* 245:5166–5168.
- Reynolds, J. A., and C. Tanford. 1970. Gross conformation of protein-sodium dodecyl sulfate complexes. *J. Biol. Chem.* 245:5161–5165.
- Reynolds, J. A., and C. Tanford. 1970. Binding of dodecyl sulfate to proteins at high binding ratios. Possible implications for the state of proteins in biological membranes. *Proc. Natl. Acad. Sci. USA.* 66:1002–1003.
- Ibel, K., R. P. May, K. Kirschner, H. Szadkowski, E. Mascher, and P. Lundahl. 1990. Protein-decorated micelle structure of sodium-dodecyl-sulfate - protein complexes as determined by neutron scattering. *Eur. J. Biochem.* 190:311–318.
- Jones, M. N. 1992. Surfactant Interactions with biomembranes and proteins. *Chem. Soc. Rev.* 21:127–136.
- Shirahama, K., K. Tsujii, and T. Takagi. 1974. Free-boundary electrophoresis of sodium dodecyl sulfate (SDS)-protein polypeptide complexes with special reference to SDS-polyacrylamide gel electrophoresis. *J. Biochem. (Tokyo).* 75:309–319.
- Mattice, W. L., J. M. Riser, and D. S. Clark. 1976. Conformational properties of the complexes formed by proteins and sodium dodecyl sulfate. *Biochemistry.* 15:4264–4272.
- Lundahl, P., E. Greijer, M. Sandberg, S. Cardell, and K. O. Eriksson. 1986. A model for ionic and hydrophobic interactions and hydrogen-bonding in sodium dodecyl sulfate-protein complexes. *Biochim. Biophys. Acta.* 873:20–26.
- Westerhuis, W. H. J., J. N. Sturgis, and R. A. Niederman. 2000. Reevaluation of the electrophoretic migration behavior of soluble globular proteins in the native and detergent-denatured states in polyacrylamide gels. *Anal. Biochem.* 284:143–152.
- Turro, N. J., X.-G. Lei, K. P. Ananthapadmanabhan, and M. Aronson. 1995. Spectroscopic probe analysis of protein-surfactant interactions: the BSA/SDS system. *Langmuir.* 11:2525–2533.
- Xu, Q., and T. A. Keiderling. 2004. Effect of sodium dodecyl sulfate on folding and thermal stability of acid-denatured cytochrome c: A spectroscopic approach. *Protein Sci.* 13:2949–2959.
- Nielsen, A. D., L. Arleth, and P. Westh. 2005. Analysis of protein-surfactant interactions: a titration calorimetric and fluorescence spectroscopic investigation of interactions between *Humicola insolens* cutinase and an anionic surfactant. *Biochim. Biophys. Acta.* 1752:124–132.
- Moosavi-Movahedi, A. A. 2005. Thermodynamics of protein denaturation by sodium dodecyl sulfate. *J. Iranian Chem. Soc.* 2:189–196.
- Moosavi-Movahedi, A. A., and A. A. Saboury. 1999. Elucidation of binding sites for protein denaturation by surfactant. *J. Chem. Soc. Pak.* 21:248–259.
- Chattoraj, D. K., S. C. Biswas, P. K. Mahapatra, and S. Chatterjee. 1999. Standard free energies of binding of solute to proteins in aqueous medium. Part 2. Analysis of data obtained from equilibrium dialysis and isopiestic experiments. *Biophys. Chem.* 77:9–25.
- Andrade, M. I. P., E. Boitard, M. A. Saghal, P. Manley, M. N. Jones, and H. A. Skinner. 1981. Enthalpy of interaction of ribonuclease A and *n*-alkyl sulfates in aqueous solution. *J. Chem. Soc. Faraday Trans.* 77:2939–2948.
- Tipping, E., M. N. Jones, and H. A. Skinner. 1974. Enthalpy of interaction between globular proteins and sodium *n*-dodecyl sulfate in aqueous solution. *J. Chem. Soc. Faraday Trans.* 70:1306–1315.
- Colton, I. J., J. D. Carbeck, J. Rao, and G. M. Whitesides. 1998. Affinity capillary electrophoresis, a physical-organic tool for studying interactions in biomolecular recognition. *Electrophoresis.* 19:367–382.
- Day, Y. S. N., C. L. Baird, R. L. Rich, and D. G. Myszkowski. 2002. Direct comparison of binding equilibrium, thermodynamic, and rate constants determined by surface- and solution-based biophysical methods. *Protein Sci.* 11:1017–1025.
- Hakansson, K., M. Carlsson, L. A. Svensson, and A. Liljas. 1992. Structure of native and apo carbonic anhydrase II and structure of some of its anion-ligand complexes. *J. Mol. Biol.* 227:1192–1204.
- Stams, T., and D. W. Christianson. 2000. X-ray crystallographic studies of mammalian carbonic anhydrase isozymes. *In* The Carbonic Anhydrases: New Horizons. W. R. Chegwidden, N. D. Carter, and Y. H. Edwards, editors. Birkhaeuser Verlag, Basel. 159–174.
- Supuran, C. T., A. Scozzafava, and A. Casini. 2003. Carbonic anhydrase inhibitors. *Med. Res. Rev.* 23:146–189.
- Carlsson, U., and B.-H. Jonsson. 1995. Folding of beta-sheet proteins. *Curr. Opin. Struct. Biol.* 5:482–487.
- Carlsson, U., and B.-H. Jonsson. 2000. Folding and stability of human carbonic anhydrase II. *In* The Carbonic Anhydrases: New Horizons. W. R. Chegwidden, N. D. Carter, and Y. H. Edwards, editors. Birkhaeuser Verlag, Basel. 241–259.
- Bushmarina, N. A., I. M. Kuznetsova, A. G. Biktashev, K. K. Turoverov, and V. N. Uversky. 2001. Partially folded conformations in the folding pathway of bovine carbonic anhydrase II: a fluorescence spectroscopic analysis. *ChemBioChem.* 2:813–821.
- Edsall, J. T., S. Mehta, D. V. Myers, and J. M. Armstrong. 1966. Structure and denaturation of human carbonic anhydrases in urea and guanidine hydrochloride solutions. *Biochemische Z.* 345:9–36.
- Fransson, C., P. O. Freskgaard, H. Herbertsson, A. Johansson, P. Jonasson, L. G. Martensson, M. Svensson, B. H. Jonsson, and U. Carlsson. 1992. *Cis-trans* isomerization is rate-determining in the reactivation of denatured human carbonic anhydrase II as evidenced by proline isomerase. *FEBS Lett.* 296:90–94.
- Ko, B. P. N., A. Yazgan, P. L. Yeagle, S. C. Lottich, and R. W. Henkens. 1977. Kinetics and mechanism of refolding of bovine carbonic anhydrase. A probe study of the formation of the active site. *Biochemistry.* 16:1720–1725.
- Montich, G. G. 2000. Partly folded states of bovine carbonic anhydrase interact with zwitterionic and anionic lipid membranes. *Biochim. Biophys. Acta.* 1468:115–126.
- Ptitsyn, O. B. 1992. The molten globule state. *In* Protein Folding. T. E. Creighton, editor. 243–300. Freeman, New York.
- Svensson, M., P. Jonasson, P.-O. Freskgaard, B.-H. Jonsson, M. Lindgren, L.-G. Maartensson, M. Gentile, K. Boren, and U. Carlsson. 1995. Mapping the folding intermediate of human carbonic anhydrase II. Probing substructure by chemical reactivity and spin and fluorescence labeling of engineered cysteine residues. *Biochemistry.* 34:8606–8620.
- Wong, K.-P., and C. Tanford. 1973. Denaturation of bovine carbonic anhydrase B by guanidine hydrochloride. Process involving separable sequential conformational transitions. *J. Biol. Chem.* 248:8518–8523.

41. Semisotnov, G. V., V. N. Uverskii, I. V. Sokolovskii, A. M. Gutin, O. I. Razgulyaev, and N. A. Rodionova. 1990. Two slow stages in refolding of bovine carbonic anhydrase B are due to proline isomerization. *J. Mol. Biol.* 213:561–568.
42. Henkens, R. W., and T. P. Oleksiak. 1991. Structural elements in unfolded carbonic anhydrase. *Carbonic Anhydrase, Proc. Int. Workshop.* 44–49.
43. Martensson, L. G., B. H. Jonsson, P. O. Freskgard, A. Kihlgren, M. Svensson, and U. Carlsson. 1993. Characterization of folding intermediates of human carbonic anhydrase II: probing substructure by chemical labeling of SH groups introduced by site-directed mutagenesis. *Biochemistry.* 32:224–231.
44. Ptitsyn, O. B. 1995. Molten globule and protein folding. *Adv. Protein Chem.* 47:83–229.
45. Wetlaufer, D. B., and Y. Xie. 1995. Control of aggregation in protein refolding: a variety of surfactants promote renaturation of carbonic anhydrase II. *Protein Sci.* 4:1535–1543.
46. Cleland, J. L., and D. I. C. Wang. 1990. Refolding and aggregation of bovine carbonic anhydrase B: quasi-elastic light scattering analysis. *Biochemistry.* 29:11072–11078.
47. Gitlin, I., K. L. Gudiksen, and G. M. Whitesides. 2005. Peracetylated bovine carbonic anhydrase (BCA-Ac<sub>18</sub>) is kinetically more stable than native BCA to sodium dodecyl sulfate. *J. Phys. Chem. B.* 110:2372–2377.
48. Gudiksen, K. L., A. R. Urbach, I. Gitlin, J. Yang, J. A. Vazquez, C. E. Costello, and G. M. Whitesides. 2004. The influence of the Zn(II) cofactor on the refolding of bovine carbonic anhydrase after denaturation with sodium dodecyl sulfate. *Anal. Chem.* 76:7151–7161.
49. Yang, J., I. Gitlin, V. M. Krishnamurthy, J. A. Vazquez, C. E. Costello, and G. M. Whitesides. 2003. Synthesis of monodisperse polymers from proteins. *J. Am. Chem. Soc.* 125:12392–12393.
50. Gudiksen, K. L., I. Gitlin, J. Yang, A. R. Urbach, D. T. Moustakas, and G. M. Whitesides. 2005. Eliminating positively charged lysine  $\epsilon$ -NH<sub>3</sub><sup>+</sup> groups on the surface of carbonic anhydrase has no significant influence on its folding from sodium dodecyl sulfate. *J. Am. Chem. Soc.* 127:4707–4714.
51. Colton, I. J., J. R. Anderson, J. Gao, R. G. Chapman, L. Isaacs, and G. M. Whitesides. 1997. Formation of protein charge ladders by acylation of amino groups on proteins. *J. Am. Chem. Soc.* 119:12701–12709.
52. Gao, J., and G. M. Whitesides. 1997. Using protein charge ladders to estimate the effective charges and molecular weights of proteins in solution. *Anal. Chem.* 69:575–580.
53. Gao, J., M. Mammen, and G. M. Whitesides. 1996. Evaluating electrostatic contributions to binding with the use of protein charge ladders. *Science.* 272:535–537.
54. Menon, M. K., and A. L. Zydney. 2000. Determination of effective protein charge by capillary electrophoresis: effects of charge regulation in the analysis of charge ladders. *Anal. Chem.* 72:5714–5717.
55. Gitlin, I., M. Mayer, and G. M. Whitesides. 2003. Significance of charge regulation in the analysis of protein charge ladders. *J. Phys. Chem. B.* 107:1466–1472.
56. Gitlin, I., J. D. Carbeck, and G. M. Whitesides. 2006. Why are proteins charged? Networks of charge-charge interactions in proteins measured by charge ladders and capillary electrophoresis. *Angew. Chem. Int. Ed. Engl.* 45:3022–3060.
57. Linderstrom-Lang, K. 1924. The ionization of proteins. *Compt. Rend. Trav. Lab. Carlsberg.* 15:1–29.
58. Reference deleted in proof.
59. Fujita, T., J. Iwasa, and C. Hansch. 1964. A new substituent constant, P, derived from partition coefficients. *J. Am. Chem. Soc.* 86:5175–5180.
60. Pliska, V., M. Schmidt, and J. L. Fauchere. 1981. Partition coefficients of amino acids and hydrophobic parameters p of their side-chains as measured by thin-layer chromatography. *J. Chromatogr.* 216:79–92.
61. Hansch, C., and E. Coats. 1970.  $\alpha$ -Chymotrypsin: case study of substituent constants and regression analysis in enzymic structure-activity relations. *J. Pharm. Sci.* 59:731–743.
62. Fersht, A. R. 1999. *Structure and Mechanism in Protein Science.* W.H. Freeman, New York.
63. Hagen, S. J., J. Hofrichter, A. Szabo, and W. A. Eaton. 1996. Diffusion-limited contact formation in unfolded cytochrome c: estimating the maximum rate of protein folding. *Proc. Natl. Acad. Sci. USA.* 93:11615–11617.
64. Chan, C. K., Y. Hu, S. Takahashi, D. L. Rousseau, W. A. Eaton, and J. Hofrichter. 1997. Submillisecond protein folding kinetics studied by ultrarapid mixing. *Proc. Natl. Acad. Sci. USA.* 94:1779–1784.
65. Semisotnov, G. V., N. A. Rodionova, V. P. Kutysenko, B. Ebert, J. Blanck, and O. B. Ptitsyn. 1987. Sequential mechanism of refolding of carbonic anhydrase B. *FEBS Lett.* 224:9–13.
66. Yazgan, A., and R. W. Henkens. 1972. Role of zinc(II) in the refolding of guanidine hydrochloride denatured bovine carbonic anhydrase. *Biochemistry.* 11:1314–1318.
67. Putnam, F., and H. Neurath. 1945. Interaction between proteins and synthetic detergents. II. Electrophoretic analysis of serum albumin-sodium dodecyl sulfate mixtures. *J. Biol. Chem.* 159:195–209.
68. Gelamo, E. L., and M. Tabak. 2000. Spectroscopic studies on the interaction of bovine (BSA) and human (HSA) serum albumins with ionic surfactants. *Spectrochim. Acta (A).* 56A:2255–2271.
69. Paz-Andrade, M. I., M. N. Jones, and H. A. Skinner. 1978. Enthalpy of interaction between some cationic polypeptides and *n*-alkyl sulfates in aqueous solution. *J. Chem. Soc. Faraday Trans.* 74:2923–2929.
70. Reference deleted in proof.
71. Hilsner, V. J., and E. Freire. 1995. Quantitative analysis of conformational equilibrium using capillary electrophoresis: applications to protein folding. *Anal. Biochem.* 224:465–485.
72. Simonson, T. 2003. Electrostatics and dynamics of proteins. *Rep. Prog. Phys.* 66:737–787.
73. Simonson, T., and C. L. Brooks III. 1996. Charge screening and the dielectric constant of proteins: insights from molecular dynamics. *J. Am. Chem. Soc.* 118:8452–8458.
74. Reference deleted in proof.
75. Dill, K. A., and S. Bromberg. 2002. *Molecular Driving Forces: Statistical Thermodynamics in Chemistry and Biology.* Garland Science, New York.
76. Gill, S. J., and I. Wadso. 1976. An equation of state describing hydrophobic interactions. *Proc. Natl. Acad. Sci. USA.* 73:2955–2958.
77. Zhou, H., and Y. Zhou. 2002. Stability scale and atomic solvation parameters extracted from 1023 mutation experiments. *Proteins.* 49:483–492.